A&A 482, 657–664 (2008)
DOI: 10.1051/0004-6361:20078265
© ESO 2008

Astronomy & Astrophysics

Constraints to Uranus' great collision IV

The origin of Prospero

M. G. Parisi[1,2,3,⋆], G. Carraro[4,5], M. Maris[6], and A. Brunini[3]

[1] Instituto Argentino de Radioastronomía (IAR), C. C. N° 5, 1894 Villa Elisa, Argentina
e-mail: gparisi@iar-conicet.gov.ar
[2] Departamento de Astronomía, Universidad de Chile, Casilla 36-D, Santiago, Chile
e-mail: gparisi@das.uchile.cl
[3] Facultad de Ciencias Astronómicas y Geofísicas, Universidad Nacional de La Plata, Argentina
e-mail: [gparisi;abrunini]@fcaglp.fcaglp.unlp.edu.ar
[4] European Southern Observatory (ESO), Alonso de Cordova 3107, Vitacura, Santiago, Chile
e-mail: gcarraro@eso.org
[5] Dipartamento di Atronomia, Universitá di Padova, Vicolo Osservatorio 2, 35122 Padova, Italy
e-mail: giovanni.carraro@unipd.it
[6] INAF, Osservatorio Astronomico di Trieste, via G.B. Tiepolo 11, 34131 Trieste, Italy
e-mail: maris@oats.inaf.it

Received 12 July 2007 / Accepted 7 January 2008

ABSTRACT

Context. It is widely accepted that the large obliquity of Uranus is the result of a great tangential collision (GC) with an Earth size proto-planet at the end of the accretion process. The impulse imparted by the GC affected the Uranian satellite system. Nine irregular satellites (irregulars) have been discovered around Uranus. Their orbital and physical properties, in particular those of the irregular Prospero, set constraints on the GC scenario.
Aims. We attempt to set constraints on the GC scenario as the cause of Uranus' obliquity as well as on the mechanisms able to generate the Uranian irregulars.
Methods. Different capture mechanisms for irregulars operate at different stages on the giant planet formation process. The mechanisms able to capture before and after the GC the Uranian irregulars are analysed. Assuming that they were captured before the GC, we calculate the orbital transfer of the nine irregulars by the impulse imparted by the GC. If their orbital transfer is dynamically implausible, they should have originated after the GC. We then investigate and discuss the dissipative mechanisms able to operate later.
Results. Very few transfers exist for five of the irregulars, which makes their existence unlikely before the GC. In particular Prospero could not exist at the time of the GC. Different capture mechanisms for Prospero after the GC are investigated. Gas drag by Uranus'envelope and pull-down capture are not plausible mechanisms. Capture of Prospero through a collisionless interaction seems to be difficult. The GC itself provides a mechanism of permanent capture. However, the capture of Prospero by the GC is a low probability event. Catastrophic collisions could be a possible mechanism for the birth of Prospero and the other irregulars after the GC. Orbital and physical clusterings would then be expected.
Conclusions. Either Prospero originated after the GC or the GC did not occur. In the former case, the mechanism for the origin of Prospero after the GC remains an open question. An observing program able to look for dynamical and physical families is needed. In the latter case, another theory to account for Uranus' obliquity and the formation of the Uranian regular satellites on the equatorial plane of the planet would be needed.

Key words. planets and satellites: general – planets and satellites: formation – solar system: formation

1. Introduction

Rich systems of irregular satellites (hereafter irregulars) of the giant planets have been discovered. Enabled by the use of large-format digital images on ground-based telescopes, new observational data have increased the known population of Jovian irregulars to 55 (Sheppard et al. 2003), the Saturnian population to 38 (Gladman et al. 2001; Sheppard et al. 2005a, 2006a) and the Neptunian population to 7 (Holman et al. 2004; Sheppard et al. 2006b). The Uranian system is of particular interest since a population of 9 irregulars (named Caliban, Sycorax, Prospero, Setebos, Stephano, Trinculo, S/2001U2: XXIV Ferdinand, S/2001U3: XXII Francisco and S/2003U3: XXIII Margaret) has been discovered around Uranus (Gladman et al. 1998, 2000; Kavelaars et al. 2004; Sheppard et al. 2005b). The discovery of these objects provides a unique window into processes operating in the young Solar System. In the particular case of Uranus, their existence may cast light on the mechanism responsible for its peculiar rotation axis (Parisi & Brunini 1997; Brunini et al. 2002, hereafter BP02).

Irregulars of giant planets are characterized by eccentric orbits, that are highly tilted to the parent planet equatorial plane, and in some case retrograde. These objects cannot have formed by circumplanetary accretion as regular satellites but they are

⋆ Member of the Carrera del Investigador Científico, Consejo Nacional de Investigaciones Científicas y Técnicas (CONICET), Argentina.

likely products of an early capture of primordial objects from heliocentric orbits, probably in association with planet formation itself (Jewitt & Sheppard 2005). It is possible for an object circling about the sun to be temporarily trapped by a planet. In terms of the classical three-body problem this type of capture can occur when the object passes through the interior Lagrangian point, L_2, with a very low relative velocity. But, without any other mechanism, such a capture is not permanent and the objects will eventually return to a solar orbit after several or several hundred orbital periods. To turn a temporary capture into a permanent one requires a source of orbital energy dissipation and that particles remain inside the Hill sphere long enough for the capture to be effective.

Although giant planets have no efficient mechanism of energy dissipation for permanent capture, at their formation epoch several mechanisms may have operated: 1) *gas drag* in the solar nebula or in an extended, primordial planetary atmosphere or in a circumplanetary disk (Pollack et al.1979; Cuk & Burns 2003), 2) *pull-down capture* caused by the mass growth and/or orbital expansion of the planet which expands its Hill sphere (Brunini 1995; Heppenheimer & Porco 1977), 3) *collisionless interactions* between a massive planetary satellite and guest bodies (Tsui 1999) or between the planet and a binary object (Agnor & Hamilton 2006), and 4) collisional interaction between two planetesimals passing near the planet or between a planetesimal and a regular satellite. This last mechanism, the so called *break-up* process, leads to the formation of dynamical groupings (e.g. Colombo & Franklin 1971; Nesvorny et al. 2004). After a break-up the resulting fragments of each progenitor would form a population of irregulars with similar surface composition, i.e. similar colors, and irregular shapes, i.e. light-curves of wide amplitude. Significant fluctuations in the light-curves of Caliban (Maris et al. 2001) and Prospero (Maris et al. 2007a) and the time dependence observed in the spectrum of Sycorax (Romon et al. 2001) suggest the idea of a break-up process for the origin of the Uranian irregulars.

Several theories to account for the large obliquity of Uranus have been proposed. Kubo-Oka & Nakazawa (1995) investigated the tidal evolution of satellite orbits and examined the possibility that the orbital decay of a retrograde satellite leads to the large obliquity of Uranus, but the large mass required for the hypothetical satellite makes this possibility very implausible. An asymmetric infall or torques from nearby mass concentrations during the collapse of the molecular cloud core leading to the formation of the Solar System could twist the total angular momentum vector of the planetary system. This twist could generate the obliquities of the outer planets (Tremaine 1991). This model has the disadvantages that the outer planets must form before the infall is complete and that the conditions for the event that would produce the twist are rather strict. The model itself is difficult to quantitatively test. Tsiganis et al. (2005) proposed that the current orbital architecture of the outer Solar System could have been produced from an initially compact configuration with Jupiter and Saturn crossing the 2:1 orbital resonance by divergent migration. The crossing led to close encounters among the giant planets, producing large orbital eccentricities and inclinations which were subsequently damped to the current value by gravitational interactions with planetesimals. The obliquity changes due to the change in the orbital inclinations. Since the inclinations are damped by planetesimal interactions on timescales much shorter than the timescales for precession due to the torques from the Sun, especially for Uranus and Neptune, the obliquity returns to small values if it is small before the encounters (Hoi et al. 2007).

Large stochastic impacts at the last stage of the planetary formation process have been proposed as the possible cause of the planetary obliquities (e.g. Safronov 1969). The large obliquity of Uranus (98°) is usually attributed to a large tangential collision (GC) between the planet and an Earth-size planetesimal at the end of the epoch of accretion (e.g. Parisi & Brunini 1997; Korycansky et al. 1990). The collision may have imparted an impulse to Uranus and allowed preexisting satellites of the planet to change their orbits. Irregulars on orbits with too large a semimajor axis escape from the system (Parisi & Brunini 1997), while irregulars with a smaller semimajor axis may be pushed to outer or inner orbits, acquiring greater or lower eccentricities depending on the initial orbital elements, the geometry of the impact and the satellite position at the moment of impact. The orbits excited by this perturbation must be consistent with the present orbital configuration of the Uranian irregulars (BP02).

In an attempt to clarify the origin of the Uranus obliquity and of its irregulars, we use the most updated information on their orbital and physical properties.

In Sect. 2, we improve the model developed in BP02 for the five Uranian irregulars known at that epoch and extend our study to the new four Uranian irregulars discovered by Kavelaars et al. (2004) and Sheppard et al. (2005b). The origin of these objects after the GC is discussed in Sect. 3, where several mechanisms for the origin of Prospero are investigated. The discussion of the results and the conclusions are presented in Sect. 4.

2. Transfer of the irregulars to their current orbits

Assuming the GC scenario, the transfers of the nine known irregulars to their current orbits are computed following the procedure developed in BP02 for the five irregulars known in 2002. We present improved calculations using a more realistic code to compute the evolution of the irregular current orbital eccentricities.

If the large obliquity of Uranus has been the result of a giant tangential impact, the orbits of preexisting satellites changed due to the impulse imparted to the planet by the collision. The angular momentum and impulse transfer to the Uranian system at impact were modeled using the Uranus present day rotational and orbital properties as imput parameters (BP02).

Just before the GC, the square of the orbital velocity v_1 of a preexisting satellite of negligible mass is given by:

$$v_1^2 = Gm_U\left(\frac{2}{r} - \frac{1}{a_1}\right), \tag{1}$$

r being the position of the satellite on its orbit at the moment of the GC, a_1 its orbital semiaxis and m_U the mass of Uranus before the impact. The impactor mass is m_i and G is the gravitational constant. After the GC, the satellite is transferred to another orbit with semiaxis a_2 acquiring the following square of the velocity:

$$v_2^2 = G(m_U + m_i)\left(\frac{2}{r} - \frac{1}{a_2}\right). \tag{2}$$

We set $v_1^2 = A\ v_e^2$ and $v_2^2 = B\ (1 + m_i/m_U)\ v_e^2$, where A and B are arbitrary coefficients ($0 < A \leq 1$, $B > 0$), v_e being the escape velocity at r before the GC.

The semiaxis of the satellite orbit before (a_1) and after (a_2) the GC verify the following simple relations:

$$a_1 = \frac{r}{2\ (1 - A)}\ ,\quad a_2 = \frac{r}{2\ (1 - B)}\ . \tag{3}$$

If $A < B$ then $a_1 < a_2$. In the special case of $B = 1$, the orbits are unbound from the system. If $A > B$ then $a_1 > a_2$, the initial orbit is transferred to an inner orbit. When $A = B$, the orbital semiaxis remains unchanged ($a_1 = a_2$).

The position r of the satellite on its orbit at the epoch of the impact may be expressed in the following form:

$$r = \frac{2\,G\,m_U}{(\Delta V)^2}\left[\frac{B' - A}{\sqrt{A}\cos\Psi \pm \sqrt{(B'-A) + A\cos^2\Psi}}\right]^2, \quad (4)$$

with $B' = B\,(1 + m_i/m_U)$. Since stochastic processes can only take place at very late stages in the history of planetary accretion (e.g. Lissauer & Safronov 1991), the GC is assumed to occur at the end of Uranus formation (e.g. Korycansky et al. 1990). The mass of Uranus after the GC, $(m_i + m_U)$, is taken as Uranus' present mass. Ψ is the angle between $\boldsymbol{\nu_1}$ and the orbital velocity change imparted to Uranus ΔV. An analytical expression for ΔV is derived in BP02 assuming that the impact is inelastic (Korycansky et al. 1990) as a function of m_i, the impact parameter of the collision b, the present rotation angular velocity of Uranus $\boldsymbol{\Omega}$, the spin angular velocity that Uranus would have today if the collision had not occurred $\boldsymbol{\Omega_0}$, and α, the angle between $\boldsymbol{\Omega}$ and $\boldsymbol{\Omega_0}$:

$$\Delta V = \frac{2R_U^2}{5b}\left[\Omega^2 + \frac{\Omega_0^2}{(1+\frac{m_i}{m_U})^2(1+\frac{m_i}{3m_U})^4} - \frac{2\Omega\Omega_0\cos\alpha}{(1+\frac{m_i}{m_U})(1+\frac{m_i}{3m_U})^2}\right]^{1/2}. \quad (5)$$

R_U is the present equatorial radius of Uranus. A collision with the core itself was necessary to impart the required additional mass and angular momentum (Korycansky et al. 1990). Since b is an unknown quantity, we take its most probable value: $b = (2/3)R_C$, where R_C is the core radius of Uranus at the moment of collision assumed to be 1.8×10^4 km (Korycansky et al. 1990; Bodenheimer & Pollack 1986). The results have a smooth dependence on the impactor mass which allows us to take $m_i \sim 1 m_\oplus$ (Parisi & Brunini 1997).

The minimum eccentricity of the orbits before the collision is given by:

$$\begin{aligned} e_{1\min} &= 2\,(1-A) - 1 \quad \text{if} \quad A \le 0.5 \\ e_{1\min} &= 1 - 2\,(1-A) \quad \text{if} \quad A > 0.5, \end{aligned} \quad (6)$$

while the minimum eccentricity of the orbits after the collision is:

$$\begin{aligned} e_{2\min} &= 2\,(1-B) - 1 \quad \text{if} \quad B \le 0.5 \\ e_{2\min} &= 1 - 2\,(1-B) \quad \text{if} \quad B > 0.5. \end{aligned} \quad (7)$$

The minimum possible value of ΔV ($\Delta V_{\min}$) is obtained from Eq. (5) for an initial period $T_0 = 20$ h ($T_0 = 2\pi/\Omega_0$) and $\alpha = 70°$ (BP02). Therefore, although simulations of solid accretion in general produce random spin orientations (e.g. Chambers 2001), we further assume $T_0 = 20$ h and $\alpha = 70°$ in order to set a maximum bound on Eq. (4). Upper bounds in a_1 (a_{1M}) and a_2 (a_{2M}) are obtained from Eq. (3) through Eqs. (4) and (5) taking $\Delta V = \Delta V_{\min}$ with $\Psi = 180°$, i.e., assuming the impact in the direction opposite to the orbital motion of the satellites and taking the positive sign of the square root in Eq. (4):

$$\begin{aligned} a_{1M} &= \frac{G\,m_U\,(B'-A)^2}{(\Delta V_{\min})^2\,(1-A)(\sqrt{B'} - \sqrt{A})^2} \\ a_{2M} &= \frac{G\,m_U\,(B'-A)^2}{(\Delta V_{\min})^2\,(1-B)(\sqrt{B'} - \sqrt{A})^2}. \end{aligned} \quad (8)$$

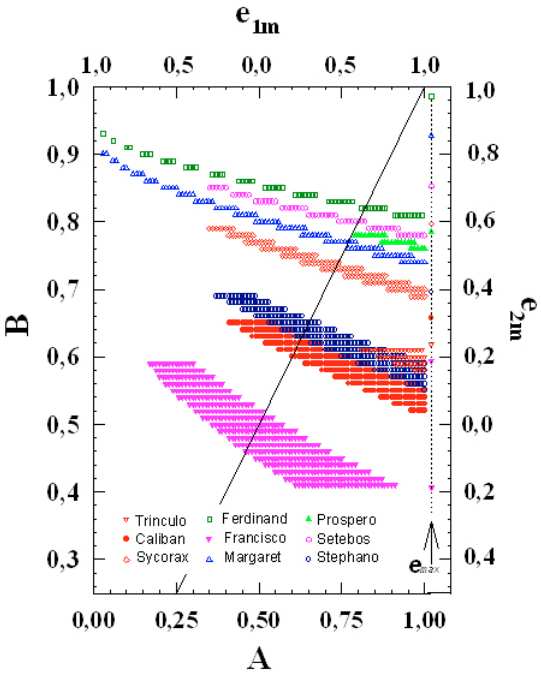

Fig. 1. The transfers capable of producing the present orbits of the Uranian irregulars. A (B) is the square of the ratio of the satellite's speed just before (after) the impact to the escape velocity at the satellite's location just before (after) the impact. e_{1m} (e_{2m}) is the minimum eccentricity of the orbits before (after) collision. The full-black line $A = B$ divides the upper region (the current orbits arise from inner orbits) and the lower region (the current orbits arise from outer orbits). The value of e_{max} tabulated in Table 2 is shown on the dashed line for comparation with e_{2m}. Trinculo: empty downward triangles, Caliban: full circles, Sycorax: empty rhombus, Ferdinand: empty squares, Francisco: full downward triangles, Margaret: empty upward triangles, Prospero: full upward triangles, Setebos: empty hexagons, Stephano: empty circles.

For each A, we calculate the value of B ($B = B'/(1 + m_i/m_U)$) corresponding to the transfer to $a_{2M} = a$, where a is the present orbital semiaxis of each of the Uranian irregulars shown in the second column of Table 1 in units of R_U. From Eq. (7), this value of B provides the minimum possible value of $e_{2\,min}$, e_{2m}, that the orbit of each irregular may acquire at impact for each initial condition A and all initial conditions for T_0, α, Ψ and m_i, i.e., if a transfer of a given orbit (A, B) is not possible for $\Psi = 180°$, $T_0 = 20$ h and $\alpha = 70°$, the same transfer (A, B) is not possible for any other incident direction of the impactor and for any other value of T_0 and α either.

Since the orbits of the irregulars are time dependent, the orbital evolution of the five Uranian irregulars known in 2002 was computed in PB02 by numerical integration of the equations of the elliptical restricted three body problem formed by the Sun, Uranus and the satellite. In this paper, we present the orbital evolution of the nine known Uranian irregulars for 10^5 yrs using the symplectic integrator of Wisdom & Holman (1991), where the perturbations of the Sun, Jupiter, Saturn and Neptune are included. The mean (e_{mean}), maximum (e_{max}) and minimum (e_{min}) eccentricities are shown in Table 2 for all the known Uranian irregulars.

The transfer of each satellite from its original orbit to the present one is possible only for those values of (A, B) which satisfy the condition $e_{2m} < e_{max}$. A satellite did not exist before the impact if it has no transfer and the satellites with the widest range of transfers are those with the highest probability of existing before the impact.

The transfers within a range of 20 R_U around each present satellite semiaxis ($a_{2M} = a \pm 20\ R_U$; a taken from Table 1) for all the Uranian irregulars are shown in Fig. 1. There are few transfers for Setebos, Ferdinand and Margaret. This makes the existence of these satellites before collision poorly probable. The only transfers for Trinculo and Prospero are close to the pericenter of an eccentric initial outer orbit ($e_{1m} > 0.58$ for Prospero and $e_{1m} > 0.62$ for Trinculo). The minimum eccentricity after collision e_{2m} for Trinculo is in the range [0.16–0.23], very close to e_{max} (0.237). This result gives a very low probability for the existence of Trinculo before the GC. For Prospero e_{2m} is in the range [0.52–0.57], $e_{2m} \sim e_{max}$ (0.571). Therefore this satellite could not exist before the GC. If the present large obliquity of Uranus was caused by a large impact at the end of its formation, Prospero had to originate after the event. Relating the origin of the outer Uranian system to a common formation process, all the Uranian irregulars probably were generated after the GC. The possible post-GC origin of Prospero and the other Uranian irregulars is discussed in the following section.

3. Origin of Prospero after the great collision

In this section, we analyze the possibility that Prospero was captured after the GC. We investigate the possible dissipative mechanisms able to produce its permanent capture taking into account that the giant impact is assumed to have occurred at late stages in the planetary accretion process.

3.1. Gas drag by Uranus' envelope

Bodenheimer & Pollack (1986) and Pollack et al. (1996) studied the formation of the giant planets by accretion of solids and gas. In their model, the so called core instability scenario, when the mass of the core of the planet has grown enough, a gaseous envelope begins to form around the core. For Uranus, its envelope extended until its accretion radius, which was ~500 R_U at the end of Uranus' formation (Bodenheimer & Pollack 1986). The formation of Uranus is completed when there is no more nebular gas to accrete. Otherwise, gas accretion by proto-Uranus would have continued towards the runaway gas accretion phase and the planet now would have a massive gaseous envelope. Bodenheimer & Pollack (1986) obtained that after the end of accretion, the radius of the envelope of proto-Uranus remained almost constant (~500 R_U) over a time scale of 10^4 yrs and then contracted rapidly to ~8 R_U in 10^5 yrs. The final contraction to the present-day planetary radius occurred on a slower timescale of 10^8 yrs.

Korycansky et al. (1990) carried out hydrodynamical calculations of the GC for a large set of initial conditions at the end of accretion. They found a sharp transition between the cases where almost all the mass of the envelope of Uranus remained after the impact and those where it was almost entirely dispersed by the impact. This implies that the impact should not have dispersed the envelope, as there would have been no nebular gas to re-accrete on the planet. They showed that the envelope reacts hydrodynamically at impact and it expands outward. After the shock the gas falls back on the core over a timescale of a few hours, the final result being a readjustment instead of a catastrophic transformation. The timescale for this hydrodynamical process is much shorter than the orbital period of the irregulars, which is of the order of years. We may then assume that the GC did not change the envelope density profile.

The extended envelope of Uranus in principle could be a source of gas allowing the capture of Prospero and the other irregulars after the GC. Assuming that the GC did not change the envelope profile, we fit from Fig. 1 of Korycansky et al. (1990) the density profile of Uranus' gaseous envelope before the GC, $\rho_g = c_{te} R^{-4}$ g cm^{-3} with $c_{te} = 10^{36}$ and R being measured in cm. It gives a nebular density of $\sim 4 \times 10^{-13}$ g cm^{-3} at the boundary of 500 R_U in agreement with the minimum mass nebula model.

As a first approximation, we compute the ratio of gas mass traversed by a body of density ρ_s and radius r_s in a characteristic orbital period P, to the mass of the body. Assuming for the body a circular orbit of radius R, we calculate the so-called β parameter (Pollack et al. 1979):

$$\beta = \frac{P}{\tau} = \frac{2\pi R \rho_g \pi r_s^2}{\frac{4}{3}\pi \rho_s r_s^3} = \frac{3\pi \rho_g R}{2\rho_s r_s}, \tag{9}$$

where τ is the characteristic timescale for changing any of the orbital parameters. For the permanent capture to occur β cannot be very small, $\beta \geq 0.04$ (Pollack et al. 1979). Using Eq. (9) and assuming a nebular density 10 times that of the minimum nebula model ($c_{te} = 10^{37}$) for an object the size of Prospero ($\rho_s = 1.5$ g cm^{-3}) and at Prospero's pericenter ($R = 278\ R_U$), $\beta \sim 9 \times 10^{-5}$, which is too small to affect the orbit of Prospero.

Following BP02, we now investigate in more detail the possible effect of gas drag on the Uranian irregulars after the GC due to Uranus' extended envelope before its contraction to its present state. Following the procedure of Adachi et al. (1976), we obtain the time variations of the eccentricity e and semiaxis a of each Uranian irregular. The drag force per unit mass is expressed in the form:

$$F = -C\rho_g v_{rel}^2, C = \frac{C_D \pi r_s^2}{2m}, \tag{10}$$

where v_{rel} is the relative velocity of the satellite with respect to the gas. In computing the satellite mass m, a satellite mean density ρ_s of 1.5 g cm^{-3} is taken for all the satellites (http://ssd.jpl.nasa.gov/?sat_phys_par). The drag coefficient C_D is ~1 and r_s is each satellite radius taken for each satellite from Table 1.

Assuming that the orbital elements are constant within one Keplerian period (the variations of a and e are very small), we consider the rates of change of the elements averaged over one period, that is:

$$\left\langle \frac{da}{dt} \right\rangle = -\frac{C}{\pi}(G(m_i + m_U)a)^{\frac{1}{2}} \int_0^{2\pi} \frac{\rho_g (e^2 + 1 + 2e\cos\theta)^{\frac{3}{2}}}{(1 + e\cos\theta)^2} d\theta,$$

$$\left\langle \frac{de}{dt} \right\rangle = -\frac{C}{\pi}\left(1 - e^2\right)$$

$$\left(\frac{G(m_i + m_U)}{a}\right)^{\frac{1}{2}} \int_0^{2\pi} \frac{\rho_g (e + \cos\theta)(e^2 + 1 + 2e\cos\theta)^{\frac{1}{2}}}{(1 + e\cos\theta)^2} d\theta. \tag{11}$$

Since after the end of accretion the gas density in the outer regions of the envelope contracts rapidly, we have integrated Eqs. (11) back in time for 10^4 yrs for the 9 Uranian irregulars. We have taken v_{rel} as the satellite orbital velocity since we have assumed a null gas velocity. This assumption maximizes the orbital damping for retrograde satellites which allows us to set upper bounds to the damping effect for the orbital eccentricity and semiaxis of all the retrograde irregulars. The mean eccentricity e_{mean} and the actual semiaxis a from Table 1 were taken as the initial conditions for the integrations. We take

Table 1. Present parameters of the Uranian irregulars and orbital damping due to gas drag exerted by Uranus extended envelope. r_s and a are the present physical radius and the present orbital semiaxis of the irregulars. e_{mean} is their calculated mean eccentricity tabulated in Table 2. a_i and e_i are the orbital semiaxis and eccentricity just after the GC, while $(\Delta a)/a_i)$ and $(\Delta e/e_i)$ are the damping of these orbital elements since the epoch of the GC until the contraction of the Uranus envelope.

Satellite	r_s[km]	$a[R_U]$	e_{mean}	$a_i[R_U]$	e_i	$(\Delta a)/a_i)$	$(\Delta e/e_i)$
Caliban	49	283	0.191	287.5	0.1973	1.602×10^{-2}	3.289×10^{-2}
Sycorax	95	482	0.541	485	0.5436	6.307×10^{-3}	4.795×10^{-3}
Prospero	15	645	0.432	648	0.4342	4.585×10^{-3}	4.997×10^{-3}
Setebos	15	694	0.581	701.8	0.5853	1.123×10^{-2}	7.366×10^{-3}
Stephano	10	314	0.251	333	0.2781	6.058×10^{-2}	0.1080
Trinculo	5	336	0.218	361.6	0.2501	7.623×10^{-2}	0.1475
Ferdinand	6	813	0.660	839.3	0.6701	3.241×10^{-2}	1.533×10^{-2}
Francisco	6	169	0.142	280.6	0.3593	0.6604	1.530
Margaret	5.5	579	0.633	649	0.6705	0.1209	5.917×10^{-2}

Table 2. Variation of the eccentricity of the Uranian irregulars due to Solar and giant planet perturbations over a period of 10^5 yrs.

Satellite	e_{mean}	e_{max}	e_{min}
Caliban	0.191	0.315	0.072
Sycorax	0.514	0.594	0.438
Prospero	0.432	0.571	0.305
Setebos	0.581	0.704	0.463
Stephano	0.251	0.381	0.121
Trinculo	0.218	0.237	0.200
Ferdinand	0.660	0.970	0.393
Francisco	0.142	0.187	0.093
Margaret	0.633	0.854	0.430

$\rho_g = c_{te}\, R^{-4}$ g cm^{-3} with $c_{te} = 10^{36}$ and $R = a(1-e^2)/(1 + e\cos\theta)$, a being measured in cm. The orbital damping is shown in Table 1, where a_i and e_i are the initial semiaxis and eccentricity just after the GC at the end of accretion and $\Delta a = (a_i - a)$ and $\Delta e = (e_i - e_{mean})$, are the damping in the orbital semiaxis and eccentricity. Stephano, Trinculo and Margaret have experienced little orbital evolution while Francisco suffered a large orbital damping (see Table 1). The permitted transfers of Fig. 1 would increase for Francisco since the condition $e_{2m} < e_i$ should be then satisfied. However, the orbital evolution of the larger satellites, in particular of Prospero, is negligible. Even increasing the nebula density by a factor of 10 ($c_{te} = 10^{37}$), the damping of the orbital elements of Prospero is too small with $\Delta a/a_i = 0.046$ and $\Delta e/e_i = 0.048$. This satellite did not experience any orbital evolution due to Uranus' extended envelope and thus could not have been captured by gas drag after the GC.

The pressure forces acting on a body traveling through the gas not only decelerates it, but also subjects it to stresses. If the stress is greater than the strength of the body, the body is fractured in fragments of different size. The fragments move away from one another since drag forces vary inversely with size and act to separate them. The average pressure on the forward hemisphere of a non-rotating, spherical body as it moves through the gas with relative velocity v_{rel} is approximately equal to the dynamic pressure, $p_{dyn} = \frac{1}{2}\rho_g v_{rel}^2$ (Pollack et al.1979). The body will fragment into pieces if $p_{dyn} \geq Q$, where Q is the compressive strength. Values of Q on the order of 3×10^6 dyne cm^{-2} are needed to shatter strong (e.g. rock/ice) targets (which is 10 times lower than the value adopted for asteroids), while compressive strength on the order of $3{\times}10^4$ dyne cm^{-2} are appropriate for relatively weak (snow-like) targets (Farinella & Davis 1996; Stern 1996). For a body on a circular orbit at the present pericenter of Prospero ($R = 278\ R_U$), where v_{rel} is the circular speed around Uranus at R and taking $c_{te} = 10^{37}$ for ρ_g, $p_{dyn} \sim 0.17$ dyne cm^{-2}, and at Sycorax's pericenter $p_{dyn} \sim 1$ dyne cm^{-2}. In both cases $p_{dyn} \ll Q$ and Prospero could not have been generated by the dynamical rupture of a parent object.

A collision may fracture the parent body but if the energy at impact is not sufficient to disperse the fragments, drag forces may act to separate them against their mutual attraction. The relative importance of these effects is measured by the ratio ϵ_j of the drag force on a given fragment j to the gravitational force acting on j by the other fragments i (Pollack et al.1979):

$$\epsilon_j = \sum_{i,i\neq j} \frac{F_{Dj} m_j}{F_{Gij} m_j}, \tag{12}$$

where F_{Gij} is the gravitational force between the particles i and j, and F_{Dj} is the drag force on the particle j of radius r_j:

$$F_{Dj} = \frac{C_D \rho_g \pi r_j^2 v^2}{\frac{8}{3}\pi\rho_s r_j^3}\,. \tag{13}$$

The fragment j is dispersed by the gas if $\epsilon_j > 1$ (Pollack et al. 1979). In order to estimate the order of magnitude of the effect, we computed Eq. (12) for j = Prospero at Prospero's pericenter taking into account the gravitational attraction due to another fragment of equal size, and at the Sycorax pericenter taking into account the gravitational force of Sycorax on Prospero. In the first case, we obtain $\epsilon_j = 10^{-5}$ and in the second case at the Sycorax pericenter $\epsilon_j = 0.04$. We then conclude that pressure forces are not strong enough either to fragment a possible parent object from which Prospero originated, or to disperse its fragments. In addition Prospero suffered no orbital evolution due to gas drag and could not have been captured by Uranus' envelope after the GC.

3.2. Pull-down capture

Within the GC scenario, runaway of the cores of the planets occurred during the first stages of accretion but stopped for each embryo after it reached a size of about 1000 km. At 10–35 AU the final mass distribution contained several hundreds of Mars-size (or larger) bodies dominating the mass of the residual disk. Beaugé et al. (2002), investigated the effects of the post-formation planetary migration on satellites orbits. They obtained that if the large-body component (composed of Mars-size bodies) dominated the mass of the residual disk, the presently accepted change in the orbit of Uranus of ~3 AU is too large and it is not compatible with the observed distribution of its satellites. Even an orbital change of ~1.5 AU already causes sufficient instabilities to eject all the Uranian irregulars. Pull-down capture

caused by the orbital expansion of the planet could then not be a plausible mechanism for the origin of Prospero and the other irregulars. Pull-down capture caused by the mass growth of the planet after the GC would not be possible given that the impact is assumed to have occurred at the end of the accretion process when there was no more mass to be accreted by the planet.

3.3. Collisionless interactions

Within the framework of the restricted three-body problem, a capture is always followed by an escape. To end up with a long term capture, the satellite has to dissipate energy in a short time. The entrance energy ΔE within the gravitational field of the planet is (Tsui 1999):

$$\Delta E = -2.15\mu^{2/3}(1-\delta)\frac{GM_\odot}{a_p}, \quad (14)$$

$\mu = M_p/M_\odot$ and $\delta \ll 1$, where M_p and a_p are the mass and orbital semiaxis of the planet.

Tsui (1999) suggested a permanent capture mechanism where a guest satellite encounters some existing inner orbit massive planetary satellite causing its velocity vector to be deflected keeping the irregular in orbit around the planet. In this way, the effective two-body potential would be about twice the entrance energy ΔE of the guest satellite. The radius R_1 of the orbit of the guest satellite after deflection is then given by:

$$R_1 = \frac{0.23}{1-\delta}\mu^{1/3}a_p. \quad (15)$$

In the case of Uranus, for a minimum entrance energy of $\delta = 0$, the minimum permanent orbital radius of the guest satellite is $R_1 = 955\ R_U$. This value of R_1 is much larger than the present semiaxis of Prospero (see Table 1), making the capture of Prospero by this mechanism implausible.

The fact that binaries have recently been discovered in nearly all the solar system's small-body reservoirs suggests that binary-planet gravitational encounters could bring a possible mechanism for irregular capture (Agnor & Hamilton 2006). One possible outcome of gravitational encounters between a binary system and a planet is an exchange reaction, where one member of the binary is expelled and the other remains bound to the planet. Tsui (1999) extended the scenario of large angle satellite-satellite scattering to the formation of the Pluto-Charon pair assuming that Pluto was a satellite of Neptune and that Charon was a guest satellite. Through Eqs. (14) and (15), the conditions for the escape of the pair was found. Following their scenario, let us consider the hypothesis that Prospero was a member of a guest binary entering Uranus' field, with energy density ΔE_{bin}, above the minimum density given by Eq. (14) and $\delta = 0$. A close encounter with Uranus could result in disruption of the binary, leading to the ejection of one member and capture of the other. The minimum semiaxis R_1 is given by Eq. (15). However, even this scenario seems to be unlikely since the semiaxis of Prospero is smaller than $955\ R_U$.

3.4. Collisional interactions: break-up processes

Collisional interactions between two planetesimals passing near the planet or between a planetesimal and a regular satellite, the so called break-up process, leads to the formation of dynamical groupings (e.g. Colombo & Franklin 1971; Nesvorny et al. 2004). The resulting fragments of each progenitor body after a break-up will form a population of irregulars expected to have similar surface composition, i.e. similar colors, and irregular shapes, i.e. large temporal variations in the light curve as these irregular bodies rotate.

The critical rotation period (T_c) at which centripetal acceleration equals gravitational acceleration for a rotating spherical object is:

$$T_c = \left(\frac{3\pi}{G\rho_{ob}}\right)^{1/2}, \quad (16)$$

where G is the gravitational constant and ρ_{ob} is the density of the object. With $\rho_{ob} = 0.5$, 1, 1.5 and 2 g cm^{-3}, $T_c = 4.7$, 3.3, 2.7 and 2.3 h, respectively. The rotation period of Prospero is about 4 h (Maris et al. 2007a), and it seems unlikely that light and dark surface markings on a spherical Prospero could be responsible for its light curve amplitude of 0.2 mag (Maris et al. 2007a). Even at longer periods, real bodies will suffer centripetal deformation into aspherical shapes. For a given density and specific angular momentum (H), the nature of the deformation depends on the strength of the object. In the limiting case of a strengthless (fluid) body, the equilibrium shapes have been well studied (Chandrasekhar 1987). For $H \leq 0.304$ [in units of $(GM^3R_{sphe})^{1/2}$], where M (kg) is the mass of the object and R_{sphe} is the radius of an equal-volume sphere, the equilibrium shapes are the oblate Maclaurin spheroids. For $0.304 \leq H \leq 0.390$ the equilibrium figures are triaxial Jacobi ellipsoids. Strengthless objects with $H > 0.390$ are rotationally unstable to fission. The Kuiper Belt objects (KBOs), being composed of solid matter, clearly cannot be strengthless. However, it is likely that the interior structures of these bodies have been repeatedly fractured by impacts, and that their mechanical response to applied rotational stress is approximately fluid-like. Such "rubble pile" structure has long been studied in the asteroid belt (Farinella et al. 1981) and in the Kuiper Disk (Sheppard & Jewitt 2002; Jewitt & Sheppard 2002; Romanishin & Tegler 1999). Farinella & Davis (1996) obtained that KBOs larger than about 100 km in diameter are massive enough to survive collisional disruption over the age of the solar system, but may nevertheless have been internally fractured into rubble piles.

Whether a collision between an impactor and a target results in growth or erosion depends primarily on the energy of the impact and the mass and strength of the target. If the mass of the impactor is small compared to the mass of the target m_s, the energy required at impact to result in a break-up is given by:

$$\frac{1}{2}m_s v_{col}^2 \geq m_s S + \frac{3}{5}\frac{Gm_s^2}{\gamma R_{ms}}, \quad (17)$$

where v_{col} is the collision speed, S is the impact strength, R_{ms} is the radius of the target and γ is a parameter which specifies the fraction of collisional kinetic energy that goes into fragment kinetic energy and is estimated to be ~0.1 (Farinella & Davis 1996). The speed of the fragments is critical when the target has a gravity field. Fragments moving slower than the local escape speed re-accumulate to form rubber pile structures.

We investigate whether Prospero could be a collisional fragment or if a collision on a primary Prospero would result in a rubber pile structure.

In computing Eq. (17), $v_{col}^2 = v_e^2 + v_{inf}^2$, where v_e is the escape speed at the target surface and v_{inf} is the typical approach velocity of the two objects at a distance large compared to the Hill sphere of the target. For two bodies colliding in the Kuiper disk, v_{inf} is given by (Lissauer & Stewart 1993):

$$v_{inf}^2 = v_k^2\left(\frac{5}{4}e^2 + i^2\right), \quad (18)$$

where v_k is the Keplerian velocity, e is the mean orbital eccentricity and i the mean orbital inclination of the KBOs. We take $\langle e \rangle = 2\langle i \rangle$ (Stern 1996). Eq. (17) was computed using Eq. (18) for values of e in the range [0.01–0.1] and orbital semiaxes of the KBOs in the range [30–60] AU. In computing the mass of the target m_s, we consider the radius R_{ms} of the KBOs in the range [10–500] km and densities between [0.5–2] g cm^{-3}. Impact strengths in the range [3×10^4–3×10^6] erg cm $^{-3}$ were taken. We obtain that targets with $R_{ms} \leq 210$ km suffer disruption for all the values of these parameters in the Kuiper Disk. Prospero has a radius of only 15 km. If Prospero originated from the Kuiper Belt, it more likely would have been a collisional fragment rather than primary body. Prospero would preserve an irregular shape after disruption since it is such small object that it is unable to become spherical because its gravity cannot overcome the material strength. Prospero could have been captured during the break-up event if the two KBOs collided within Uranus' Hill sphere, which could be possible for a minimum orbital eccentricity of the original KBOs of 0.37.

We also consider the case in which the target is a satellite of Uranus that collides with a KBO that enters the Hill sphere of the planet. Equation (17) remains valid but the following expression of v_{inf} is considered:

$$\boldsymbol{v}_{inf} = \boldsymbol{v}_{ip} - \boldsymbol{v}_{sp}, \tag{19}$$

where $\boldsymbol{v}_{ip}$ is the velocity of the KB0 with respect to Uranus and $\boldsymbol{v}_{sp}$ is the satellite orbital velocity, at the epoch of the event. We assume that the satellite orbital velocity is circular. In order to derive bounds in the relative velocity, we take two values of v_{inf}, $v_{inf} = v_{ip} \pm v_{sp}$. For v_{ip}, we assume that the KBO describes a hyperbolic orbit around Uranus during the approach giving:

$$v_{inf}^2 = \frac{2G(m_i + m_U)}{a_s} + \frac{GM_\odot}{a_{kb}}, \tag{20}$$

where we assumed $G\, M_\odot / a_{kb}$ as the relative velocity between the KBO and Uranus far from the encounter, $(m_i + m_U)$ is the present mass of Uranus and a_s the orbital semiaxis of the satellite. We calculate Eq. (17) using Eqs. (19) and (20) for a_{kb} in the range [20,60] AU and a_s [100–700] R_U for the same values of S, R_{ms} and densities we have used for the collisions between KBOs. We obtain that for all the possible parameters, any Uranus satellite with radius $R_{ms} \leq 1000$ km suffers disruption if it collides with a KBO larger than 10 km. This process would lead to the formation of two clusters of irregulars, one associated with the preexisting satellite and the other with the primary KBO. This process has the disadvantage that it is unlikely that the preexisting satellite was formed from a circumplanetary disk as regular satellites given the large orbital semiaxis required for this object.

Break-up processes predict orbital clustering. However, no obvious dynamical groupings are observed at the irregulars of Uranus. A further intensive search for more faint irregulars around Uranus is needed in order to look for dynamical and physical families.

3.5. The CG itself as a possible capture mechanism

We now turn to the question of whether the GC itself could have provided a capture mechanism (BP02). Since all the transfers with $A > B'$ lead to a more bound orbit, this process might transform a temporary capture into a permanent one (see Sect. 2 and Fig. 1). Moreover, a permanent capture could even occur from a heliocentric orbit (transfers with $A = 1$).

It is interesting to estimate the number of objects N in heliocentric orbits at the time of the GC, at distances from Uranus less than or equal to 300 R_U. Assume that the GC occurred when Uranus was almost fully formed, meaning that its feeding zone was already depleted of primordial planetesimals. We assume that the objects passing near Uranus at that time were mainly escapees from the Kuiper belt. Using the impact rate onto Uranus and the distributions of velocities and diameters given by Levison et al. (2000), and assuming that the mass in the transNeptunian region at the end of the Solar System formation was 10 times its present mass, a back-of-the-envelope calculation gives one object of diameter $D \geq 20$ km passing at a distance $R \leq 300\ R_U$ from Uranus every 6 yrs at the end of accretion (BP02). The typical crossing time T_C among protoplanets in the outer Solar System is larger than one millon years (Zhou et al. 2007). The number of objects passing near Uranus during a timescale T_C is then 167 000, which gives a probability of 6×10^{-6} for the capture of an object at about 300 R_U by the GC. This low rate of incoming objects makes the possibility of the capture of all the irregulars from heliocentric orbits difficult. Even the capture of a single object, Prospero (note that Prospero could not have an orbit bound to the planet before the GC), turns out to be of low probability. Since temporary capture can lengthen the time that a passing body can spend near the planet, a more plausible situation arises if we assume that the GC could produce the permanent capture of one or more parent objects which were orbiting temporarily around Uranus, the present irregulars being the result of a collisional break-up occurring after the GC.

4. Discussion and conclusions

It is usually believed that the large obliquity of Uranus is the result of a great tangential collision (GC) with an Earth-sized proto-planet at the end of the accretion process. We have calculated the transfer of angular momentum and impulse at impact and have shown that the GC had strongly affected the orbits of Uranian satellites. We calculate the transfer of the orbits of the nine known Uranian irregulars by the GC. Very few transfers exist for five of the nine irregulars, making their existence before the GC hardly expected. In particular, Prospero could not have existed at the time of the GC. Then, either Prospero had to originate after the GC or the GC did not occur, in which case another theory able to explain Uranus' obliquity and the formation of the Uranian regular satellites would be needed. It is usually believed that the regular satellites of Uranus have accreted from material placed into orbit by the GC (Stevenson et al. 1986).

Within the GC scenario, several possible mechanisms for the capture of Prospero after the GC were investigated. If the Uranian irregulars belong to individual captures and relating the origin of the outer uranian system to a common formation process, gas drag by Uranus' envelope and pull-down capture seem to be implausible. Three-body gravitational encounters might be a source of permanent capture. However, we found that the minimum permanent orbital radius of a guest satellite of Uranus is ~955 R_U while the current semiaxis of Prospero is 645 R_U. The GC itself could provide a mechanism of permanent capture and the capture of Prospero could have occurred from a heliocentric orbit as is required within the GC scenario, but due to the low rate of incoming objects it turns out to be difficult. Break-up processes could be the mechanism for the origin of Prospero and the other irregulars in different scenarios. Prospero might be a fragment of a primary KBO fractured by a collision with another KBO. The fragment could have been captured by Uranus if the two KBOs had a minimum orbital eccentricity of 0.37. Prospero could be a secondary member of a collisional family generated

by the collision between another satellite of Uranus and a KBO where the parent satellite of Prospero could have been captured by any mechanism before or after the GC. This process has the disadvantage that it is unlikely that the preexisting satellite was formed from a circumplanetary disk like regular satellites given the large orbital semiaxis required for this object. Since collisional scenarios require in general high collision rates, perhaps the irregulars were originally much more numerous than now. Then, Prospero and also the other irregulars might be the result of mutual collisions between hypothetical preexisting irregulars (Nesvorny et al. 2003, 2007) which could have been captured by any other mechanism before the GC.

The knowledge of the size and shape distribution of irregulars is important to know their relation to the precursor Kuiper Belt population. It could give valuable clues to determine whether they are collisional fragments from break-up processes occuring at the Kuiper Belt and thus has nothing to do with how they were individually captured later by the planet, or if they are collisional fragments produced during or after the capture event (Nesvorny et al. 2003, 2007). The differential size distribution of the Uranian irregulars approximates a power law with an exponent $q = 1.8$ (Sheppard et al. 2005b). If we assume that the size distribution of the nine irregulars with radii greater than 7 km extends down to radii of about 1 km, we would expect about 75 irregulars of this size or larger (Sheppard et al. 2005b).

The nuclei of Jupiter family comets are widely considered to be kilometer- sized fragments produced collisionally in the Kuiper Belt (Farinella & Davis 1996). Jewitt et al. (2003) compared the shape distribution of cometary nuclei in the Jupiter family with the shape distribution of small main-belt asteroids of similar size (1–10 km) and with the shape distribution of fragments produced in laboratory impact experiments. They found that while the asteroids and laboratory impact fragments show a similar distribution of axis ratio ($\langle b/a \rangle \sim 0.7$), cometary nuclei are more elongated ($\langle b/a \rangle \sim 0.6$). They predict that if comets reflect their collisional origin in the Kuiper Belt followed by sublimation-driven mass loss once inside the orbit of Jupiter, small KBOs should have average shapes consistent with those of collisionally produced fragments (i.e., $\langle b/a \rangle \sim 0.7$). To date, constraints on the shapes of only the largest KBOs are available. Prospero being slightly larger than cometary nuclei, displays a variability of 0.21 mag in the R band (Maris et al. 2007a). This corresponds to an axis ratio projected onto the plane of the sky, b/a of 0.8. The knowledge of the size and shape distribution of irregulars would shed light on the size and shape distribution of small KBOs as well as on the irregular capture mechanism.

Colors are an important diagnostic tool to unveil the physical status and the origin of the Uranian irregulars. In particular it would be interesting to assess whether it is possible to define subclasses of irregulars color, and comparing colors of these bodies with colors of minor bodies in the outer Solar System. Literature data show a dispersion in the published values that is larger than the quoted errors for each Uranian irregular (Maris et al. 2007a, and references therein). We have concluded in Maris et al. (2007a) that the Uranian irregulars are slightly red but they are not as red as the reddest KBOs.

An intensive search for fainter irregulars and a long term program of observations to recover in a self consistent manner lightcurves, colors and phase effect information is needed.

Acknowledgements. M.G.P. research was supported by Instituto Argentino de Radioastronomía, IAR-CONICET, Argentina and by Centro de Astrofísica, Fondo de Investigación avanzado en Areas Prioritarias, FONDAP number 15010003, Chile. M.M. acknowledges FONDAP for finantial support during a visit to Universidad de Chile. Part of the work of MM has been supported by INAF FFO-*Fondo Ricerca Libera* – 2006. A.B. research was supported by IALP-CONICET. We appreciate the useful suggestions by the reviewer, which have helped us to greatly improve this paper.

References

Adachi, I., Hayashi, C., & Nakazawa, K. 1976, Prog. Theo. Phys., 56, 1756
Agnor, C. B., & Hamilton, D. P. 2006, Nature, 441, 192
Beaugé, C., Roig, F., & Nesvorný, D. 2002, Icarus, 158, 438
Bodenheimer, P., & Pollack, J. B. 1986, Icarus, 67, 391
Brunini, A., & Conicet, P. 1995, Earth, Moon, and Planets, 71, 281
Brunini, A., Parisi, M. G., & Tancredi, G. 2002, Icarus, 159, 166
Chambers, J. E. 2001, Icarus, 152, 205
Chandrasekhar, S. 1987, Ellipsoidal Figures of Equilibrium (New York: Dover)
Colombo, G., & Franklin, F. A. 1971, Icarus, 15, 186
Cuk, M., & Burns, J. A. 2003, Icarus, 167, 369
Farinella, P., & Davis, D. R. 1996, Science, 273, 938
Farinella, P., Paolicchi, P., Tedesco, E. F., & Zappala, V. 1981, Icarus, 46, 114
Gladman, B. J., Nicholson, P. D., Burns, J. A., et al. 1998, Nature, 392, 897
Gladman, B. J., Kavelaars, J. J., Holman, M., et al. 2000, Icarus, 147, 320; erratum 148, 320
Gladman, B. J., Kavelaars, J. J., Holman, M., et al. 2001, Nature, 412, 163
Grav, T., Holman, M. J., & Fraser, W. 2004, APJ, 613, L77
Heppenheimer, T. A., & Porco, C. 1977, Icarus, 30, 385
Hoi Lee, M., Peale, S. J., Pfahl, E., & Ward, W. R. 2007, Icarus, in press
Holman, M.J., Kavelaars, J. J., Grav, T., et al. 2004, Nature, 430, 865
Jewitt, D., & Sheppard, S. 2002, AJ, 123, 2110
Jewitt, D., & Sheppard, S. 2005, Space Sci. Rev., 116, 441
Jewitt, D., Sheppard, S., & Fernandez, Y. 2003, AJ, 125, 3366
Kavelaars, J. J., et al. 2004, Icarus, 169, 474
Korycansky, D. G., Bodenheimer, P., Cassen, P., & Pollak, J. B. 1990, Icarus, 84, 528
Kubo-Oka, T., & Nakazawa, K. 1995, Icarus, 114, 21
Levison, H. F., Duncan, M. J., Zahnle, K., Holman, M., & Dones, L. 2000, Icarus, 143, 415
Lissauer, J. J., & Safronov, V. 1991, Icarus, 93, 288
Lissauer, J. J., & Stewart, G. R. 1993, Protostars and planets III, 1061
Luu, J., & Jewitt, D. 1996, AJ, 112, 2310
Maris, M., Carraro, G., Cremonese, G., & Fulle, M. 2001, AJ, 121, 2800
Maris, M., Carraro, G., & Parisi, M. G. 2007a, A&A, 472, 311
Maris, M., Carraro, G., & Parisi, M. G. 2007b, Proceedings of the workshop, Mutual Events of the Uranian Satellites in 2007–2008 and further observations in network, Paris, 2006, in press
Nesvorny, D., Alvarellos, J. L. A., Dones, L., & Levison, H. 2003, AJ, 126, 398
Nesvorny, D., Beaugé, C., & Dones, L. 2004, AJ, 127, 1768
Nesvorny, D., Vokrouhlický, D., & Morbidelli, A. 2007, AJ, 133, 1962
Parisi, M. G., & Brunini, A. 1997, Planetary Space Sci., 45, 181
Pollack, J. B., Burns, J. A., & Tauber, M. E. 1979, Icarus, 37, 587
Pollack, J. B., Hubickyj, O., Bodenheimer, P., et al. 1996, Icarus, 124 62
Romanishin, W., & Tegler, S. C. 1999, Nature, 398, 129
Romon, J., de Bergh, C., Barucci, M. A., et al. 2001, A&A, 376, 310
Safronov, V. S. 1969, Evolution of the Protoplanetary Cloud and Formation of The Earth and the Planets, NASA TTF-677
Sheppard, S. S., & Jewitt, D. C. 2002, AJ, 124, 1757
Sheppard, S. S., & Jewitt, D. C. 2003, Nature, 423, 261
Sheppard, S. S., Jewitt, D. C., & Marsden, B. G. 2005a, MPEC 2005-J13
Sheppard, S. S., Jewitt, D. C., & Kleyna, J. 2005b, AJ, 129, 518
Sheppard, S. S., Jewitt, D. C., Kleyna, J., & Marsden, B. G. 2006a, IAU Circ., 8727
Sheppard, S. S., Jewitt, D. C., & Kleyna, J. 2006b, AJ, 132, 171
Stevenson, D. J., Harris, A. W., & Lunine, J. I. 1986, in Satellites, ed. J. A. Burns, & D. M. S. Matthews (Tucson: Univ. of Arizona Press), 39
Stern, S. A. 1996, A&A, 310, 999
Tremaine, S. 1991, Icarus, 89, 85
Tsiganis, K., Gomes, R., Morbidelli, A., & Levison, H. F. 2005, Nature, 435, 459
Tsui, K. H. 1999, Planet Space Sci., 47, 917
Wisdom, J., & Holman, M. 1991, AJ, 102, 1528
Zhou, J.-L., Lin, D. N. C., & Sun, Y.-S. 2007, AJ, 666, 423